

Interacting Fermi gas in a harmonic trap

G. M. Bruun and K. Burnett

Department of Physics, Clarendon Laboratory, University of Oxford, Oxford OX1 3PU, England
(August 2, 2018)

In view of ongoing experiments to trap ultracold spin-polarized ${}^6\text{Li}$, we study various properties of an interacting Fermi gas in a harmonic trap taking the discrete nature of the unperturbed harmonic trap levels into account exactly. As ${}^6\text{Li}$ has a rather large and negative scattering length, we focus on the effects of the attractive atom-atom interaction on several thermodynamic properties and on the momentum and density distributions. The dependence of the chemical potential, the specific heat and the density and momentum distributions on the number of particles in the trap is obtained. We also calculate the energy of the gas. Comparison is made with results of a semiclassical calculation and with the properties of a non-interacting gas. We find that the effect of the interactions is rather large for realistic trap frequencies. Hence, it is important to include these interactions in any quantitative predictions relevant for experiments.

I. INTRODUCTION

Recently there has been a lot of interest in the properties of trapped ultra-cold atoms. This interest has largely been sparked by the achievement of Bose-Einstein condensation in the Bosonic systems ${}^{87}\text{Rb}$, ${}^7\text{Li}$, and ${}^{23}\text{Na}$ [1–3]. Several theoretical studies of trapped degenerate Fermi gases have been presented in addition to those on Bose systems. It has even been shown that a two-component gas of spin-polarized atomic ${}^6\text{Li}$ becomes superfluid at experimentally obtainable densities and temperatures [4]. This is due to the fact that ${}^6\text{Li}$ has an anomalously large and negative s -wave scattering length a , with a recent measurement giving $a \simeq -2160a_0$ where a_0 is the Bohr radius [5]. s -wave scattering is forbidden for two fermions in the same spin-state, but, the ${}^6\text{Li}$ atom has six hyperfine states. This means that by trapping ${}^6\text{Li}$ in two different hyperfine states, one can observe the relatively strong interactions due to s -wave scattering between atoms in different states. The trapping can be achieved since the energy of the hyperfine states depend on the external magnetic field. The highest three states “prefer” a lower magnetic field and can therefore be trapped in a static magnetic trap. In particular, one can trap the two highest states as proposed by Houbiers *et al* [6]. These two states will here be labeled $|\uparrow\rangle$ and $|\downarrow\rangle$. In such a two-component gas of trapped spin-polarized ${}^6\text{Li}$ atoms, there will only be, to a good approximation, interactions between atoms in different hyperfine states, whereas there will be almost no interaction between atoms in the same state. Indeed, it was for such a two-component system that the relatively high transition temperature T_c for a BCS-type phase transition was predicted [4].

The purpose of this paper is to examine the normal state properties of such a trapped gas of ${}^6\text{Li}$ atoms with components in the two highest hyperfine states. It is clearly necessary to understand these properties in the path to achieving the predicted BCS-type transition. The normal state properties of a non-interacting trapped cloud of fermions have been treated within the semiclassical Thomas-Fermi approximation [7] and also by taking the discrete nature of the trap energy levels in the non-interacting limit into account [8]. As the interactions between ${}^6\text{Li}$ atoms in two different hyperfine states are relatively strong, it is important to include the effect of these interactions in any realistic treatment of the system. Hence, the present paper extends the analysis of Refs. [7,8] by including both the discrete nature of the trap levels as well as the effects of the interactions (in the mean-field approximation).

The paper is organized as follows. In Sec. II we set up the formalism needed to treat an interacting two-component system of fermions within the mean-field approximation. We then, in Sec. III, analyze the influence of the trap potential and the interactions on the chemical potential of the gas. We show, that the interactions have two distinct effects on the chemical potential: they lower its value below the non-interacting value and smooth out the steplike features predicted by Schneider and Wallis [8]. The quasiparticle energy spectra and wave functions are considered in Sec. IV and in Sec. V we investigate the behaviour of the energy and the heat capacity. We find that at sufficiently low temperatures the interactions change the qualitative behaviour of the heat capacity. This is explained in terms of the effect the interactions have on the quasiparticle spectrum. In Sec. VI we discuss the density and momentum distribution and their deviations from the non-interacting case and from the Thomas-Fermi predictions. Finally, we summarize the results in Sec. VII.

II. FORMALISM

We consider a dilute gas of interacting ${}^6\text{Li}$ atoms in two hyperfine states trapped in an external potential $U_0(\mathbf{r})$. As the gas is dilute the interactions mainly happen through two-body collisions. Furthermore, since the s-wave scattering length is much larger than the p-wave scattering length we can neglect any interaction between fermions in the same hyperfine state. The gas is then described by the Hamiltonian:

$$\hat{H} = \sum_{\sigma} \int d^3r \psi_{\sigma}^{\dagger}(\mathbf{r}) \left[\frac{-\hbar^2}{2m} \nabla^2 + \frac{1}{2} m \omega^2 r^2 - \mu \right] \psi_{\sigma}(\mathbf{r}) - g \int d^3r \psi_{\uparrow}^{\dagger}(\mathbf{r}) \psi_{\downarrow}^{\dagger}(\mathbf{r}) \psi_{\downarrow}(\mathbf{r}) \psi_{\uparrow}(\mathbf{r}), \quad (1)$$

where m is the mass of the particles, the attractive interparticle potential has been approximated by a contact potential $V(\mathbf{r}' - \mathbf{r}) \simeq -g\delta(\mathbf{r}' - \mathbf{r})$, $g > 0$. The field operators $\psi_{\sigma}(\mathbf{r})$ obey the usual fermionic anticommutation rules and describe the annihilation of a fermion at position \mathbf{r} in the hyperfine state $|\sigma\rangle$. The trapping potential is for simplicity assumed to be well described by an isotropic harmonic oscillator $U_0(\mathbf{r}) = \frac{1}{2} m \omega^2 r^2$. The trapping frequency ω is taken to be the same for each hyperfine state. We have assumed that number of particles N in each state is the same such that we only have one chemical potential μ . As the critical temperature for a BCS type transition is maximum when the number of particles in the two hyperfine levels is equal [4,6], we expect this configuration to have the most experimental relevance. The non-interacting case is achieved by setting $g = 0$; this limit has been treated by Butts and Rokhsar within the Thomas-Fermi approximation [7] and by Schneider and Wallis [8] taking the quantizing effect of the trap potential into account. In this paper, we are interested in the effect of the interactions on the normal state properties of the gas. We can, therefore, ignore any pairing correlations leading to a BCS type transition and use the following mean-field Hamiltonian:

$$\hat{H}_{Mean} = \sum_{\sigma} \int d^3r \psi_{\sigma}^{\dagger}(\mathbf{r}) \left[\frac{-\hbar^2}{2m} \nabla^2 + \frac{1}{2} m \omega^2 r^2 + U(\mathbf{r}) - \mu \right] \psi_{\sigma}(\mathbf{r}). \quad (2)$$

Here the self-consistent field $U(\mathbf{r}) = -g\langle\psi_{-\sigma}^{\dagger}(\mathbf{r})\psi_{-\sigma}(\mathbf{r})\rangle$ is the standard Hartree-Fock result for a contact interaction. To include all two-body scattering processes on the mean-field level, one can put $g = 4\pi|a|\hbar^2/m$, with a being the s-wave scattering length of collisions between the fermions in the two hyperfine states [9]. As the trapping potential is assumed to be isotropic, the self-consistent solution of the mean-field Hamiltonian with the lowest energy will be spherically symmetric. The Hamiltonian can then readily be diagonalized by writing the field operator as $\psi_{\sigma}(\mathbf{r}) = \sum_{\nu lm} u_{lm}^{\nu}(\mathbf{r}) a_{\sigma lm}^{\nu}$. The operator $a_{\sigma lm}^{\nu}$ describes the annihilation of a quasiparticle in the hyperfine state σ with total angular momentum $[l(l+1)\hbar^2]^{1/2}$, a component along an arbitrary z-direction of $m\hbar$ and a wave function $u_{lm}^{\nu}(\mathbf{r})$. We write the quasiparticle wave function in the form

$$u_{lm}^{\nu}(\mathbf{r}) = \frac{u_l^{\nu}(r)}{r} Y_{lm}(\theta, \phi), \quad (3)$$

where $Y_{lm}(\theta, \phi)$ are the usual orbital angular momentum eigenfunctions. \hat{H}_{Mean} is then diagonalized by solving

$$E_l^{\nu} u_l^{\nu}(r) = \left[-\frac{\hbar^2 \partial_r^2}{2m} + \frac{\hbar^2 l(l+1)}{2mr^2} + \frac{1}{2} m \omega^2 r^2 + U(r) - \mu \right] u_l^{\nu}(r) \quad (4)$$

for each angular momentum l . Here the quasiparticle energy E_l^{ν} is independent of m due to the spherical symmetry. The self-consistent potential is determined by

$$U(r) = -g \sum_{\nu lm} |u_{lm}^{\nu}(\mathbf{r})|^2 f(E_l^{\nu}) = -g \sum_{\nu l} \frac{u_l^{\nu}(r)^2}{r^2} \frac{2l+1}{4\pi} f(E_l^{\nu}) \quad (5)$$

where $f(x) = 1/[\exp(x/k_B T) + 1]$ is the Fermi function and the addition theorem for spherical harmonics has been used. Numerically, we use a cutoff of the order $E_l^{\nu} \lesssim 2\mu$ for the sum given in Eq. (5). This is more than sufficient since we in this paper are considering low temperatures ($k_B T < \hbar\omega$) and we know that levels with energies higher than a few $k_B T$ give a vanishing contribution to the density. Thus, within the mean-field approximation, the problem of an interacting gas of fermions in two hyperfine states in an isotropic harmonic trap is equivalent to solving Eq. (4)-(5) self-consistently. Once a solution is found, one can easily calculate various observables for the gas. The total energy E for the particles in both hyperfine states is given by

$$\begin{aligned}
E &= \langle \hat{H} \rangle + 2\mu N \\
&= 2 \sum_{\nu l} (2l+1) f(E_l^\nu) \int d^3r u_{i0}^\nu(\mathbf{r}) \left(\frac{-\hbar^2}{2m} \nabla^2 + \frac{1}{2} m \omega^2 r^2 \right) u_{i0}^\nu(\mathbf{r}) - \frac{1}{g} \int d^3r U(r)^2.
\end{aligned} \tag{6}$$

Here we have added $2N$ to $\langle \hat{H} \rangle$ as it is the total number of particles in the trap. In the following sections we will solve the above equations for various sets of parameters and calculate several observables from the solutions.

As the negative scattering length introduces an attractive interatomic potential, the system can collapse to a fluid or solid state when the density of particles becomes too large. This effect has been examined by Houbiers *et al.* [6] within the semiclassical Thomas-Fermi approximation. For a trap with an equal number of particles in each hyperfine state they find, that the spinodal point is given by $N^{1/6}|a|/l \simeq 0.66$ with $l = \sqrt{\hbar/\omega m}$ being the trap length. Numerically, this transition is seen from the fact that there is no self-consistent solution to Eq. (4)-(5) when the chemical potential is too high for a given coupling strength. The density of particles increases for each iteration without bound indicating that the system is collapsing into a new dense phase. We find that this problem arises in the region of parameters where $N^{1/6}|a|/l \sim O(1)$ in qualitative agreement with Houbiers *et al.* However, due to the computation load we have not been able to verify in detail the prediction $N^{1/6}|a|/l \simeq 0.66$ for the spinodal transition line. As we do not have an appropriate theory for such a phase we will in this paper work with parameters (N, g) such that we are well below this spinodal phase-transition line.

We shall compare some of our results obtained from the solution of Eq. (4)-(5) with approximate results based on the Thomas-Fermi approximation. This approximation essentially treats the trap potential as being locally constant. The Hartree-Fock equations are then trivially solved for each \mathbf{r} by plane waves. The quasiparticle energies are given by

$$E_k(r) = \frac{\hbar^2 k^2}{2m} - g\rho(r) - \mu(r). \tag{7}$$

Here the local chemical potential is $\mu(r) \equiv \mu - \frac{1}{2}m\omega^2 r^2$ and the density is given by

$$\rho(r) = \int \frac{d^3k}{(2\pi)^3} f[E_k(r)]. \tag{8}$$

Eq. (7)-(8) has to be solved self-consistently at each point \mathbf{r} . The total number of particles in a single hyperfine state in the system is then $N = \int d^3r \rho(r)$.

III. THE CHEMICAL POTENTIAL

In this section we will determine the chemical potential μ as a function of the number of particles in the trap. Schneider and Wallis [8] have done an extensive analysis of $\mu(N)$ in the case of a non-interacting gas. They found some remarkable steplike features in $\mu(N)$ as compared to the Thomas-Fermi approximation; these steps were due to the shell structure of the energy spectrum of an isotropic harmonic trap. They did, however, predict that for a *real* Fermi gas, the interactions would tend to smooth out the steps. Using the formalism outlined above, we are now able to examine in detail how the interactions affect these steplike features. In Fig. (1) we have plotted the chemical potential μ as a function of the number of particles N in a single hyperfine state for various coupling strengths g for a very low temperature ($k_B T \ll \hbar\omega$). These curves were obtained by solving Eq. (4)-(5) for varying μ and g . The dashed lines correspond to the Thomas-Fermi approximation obtained from the solution of Eq. (7)-(8). In Fig. (1) (a) we have compared $\mu(N)$ for the rather large coupling strengths $g' = 1$ and $g' = 2$ with the $g = 0$ case when there are relatively few particles in the trap in order to highlight the steplike features. We have defined $g' \equiv g/(\hbar\omega l^3)$. As can be seen, that the interaction has two effects. First of all, it lowers the value of the chemical potential for a given number of particles N as compared to the $g = 0$ case. This is as expected, since the mutual attraction between the particles in the two hyperfine states lowers the energy of the gas. Secondly, we note that the step like features of $\mu(N)$ are smoothed out by the interaction. For $g' = 1$ the step like features survive up to $N \lesssim 2000$ and for $g' = 2$ they survive for $N \lesssim 500$. Fig. (1) (b) show $\mu(N)$ for $g' = 0.4$ and $g' = 0.2$. Putting $|g| = 4\pi|a|\hbar^2/m$, with $a = -2160a_0$ being the s-wave scattering length for ${}^6\text{Li}$, $g' = 0.4$ corresponds to a trap frequency of $\nu = \omega/2\pi = 144\text{Hz}$ and $g' = 0.2$ to a trap frequency of $\nu = \omega/2\pi = 288\text{Hz}$. These values are close to the ones used in the Bose-Einstein condensation experiments at JILA [10] and at MIT [11] respectively. We again see the same behaviour as in Fig. (1) (a). The step like features break down for $N \approx 4 \times 10^4$ for $g' = 0.4$. For $g' = 0.2$ they break down at $N \approx 10^5$ which is not shown in Fig. (1).

IV. THE ENERGY SPECTRUM

From Fig (1) we see, that the step like features survive even though the value of $\mu(N)$ is several $\hbar\omega$ lower than the $g = 0$ prediction. This is somewhat surprising as the steps are associated with the gaps of size $\hbar\omega$ in the $g = 0$ spectrum. One might expect these gaps to disappear once the levels are lowered by more than $\hbar\omega$ due to the interactions. To examine this effect, we have in Fig. (2) plotted the quasiparticle spectrum for $g' = 2$ for a very low temperature for each angular momentum l . In Fig. (2) (a) the chemical potential is $\mu/\hbar\omega = 8$ whereas $\mu/\hbar\omega = 13$ in Fig. (2) (b). The x-axis denotes the angular momentum l of the quasiparticle states and the quasiparticle energies are marked by the symbol \times . For comparison the symbols \circ denote the non-interacting quasiparticle energies. The chemical potential is indicated by a thin dotted line. In the non-interacting case ($g = 0$), the energy spectrum is given by $E_\nu = (\nu + 3/2)\hbar\omega$ with $\nu = 0, 1, 2, \dots$. The degeneracy of each level is $D_\nu = (\nu + 1)(\nu + 2)/2$ corresponding to the angular momentum l being $l = 0, 2, \dots, \nu$ for ν even and $l = 1, 3, \dots, \nu$ for ν odd. This degeneracy in l gives rise to the shell structure of the spectrum which is indicated in Fig. (2) by horizontal dashed lines. In the interacting case, the energy E_l^ν in general depends on both ν and l . From Fig. (2) (a) ($\mu = 8\hbar\omega$) we see, that the quasiparticle energies in the interacting case are lowered several $\hbar\omega$ as compared to the normal state energies; e.g. the lowest energy is $-1.7\hbar\omega$ for $g' = 2$ as compared to $1.5\hbar\omega$ for $g' = 0$. However, from the solid lines in Fig. (2) (a) we see, that the energies still depend only weakly on the angular momentum l . This means that the Hartree potential lowers the energy of the $l = \nu$ state by almost the same amount as it lowers the $l = 0$ (ν even) or $l = 1$ (ν odd) state. This is not *a priori* obvious as the wave functions for those two states are completely different. This is shown in Fig. (3) where the solid lines denote the quasiparticle wave functions $u_{l=0}^{\nu=8}(r)$ (a) and $u_{l=8}^{\nu=8}(r)$ (b) for $\mu = 8\hbar\omega$ and $g' = 2$. These states have the energies $E_{l=0}^{\nu=8} = 8.2\hbar\omega$ and $E_{l=8}^{\nu=8} = 8.4\hbar\omega$ respectively. The $l = 0$ wave function is spread out from $r = 0$ to $r \approx r_{class} = \sqrt{2E_n/m\omega^2} = 4l$ whereas the $l = \nu$ wave function is peaked around $r \approx 2.8l$. Hence one might expect that the Hartree potential, which is also plotted as a solid line in Fig. (3) (c), would affect the quasiparticle states completely differently. But in fact, the lowering of the two energies as compared to the $g = 0$ case is approximately the same. This explains the fact depicted in Fig. (1) that even though the chemical potential is several $\hbar\omega$ below the $g = 0$ prediction, $\mu(N)$ still exhibits the step like features. The reason is, that even though each quasiparticle energy is lowered several $\hbar\omega$ due to the interaction, there is still an approximate l -degeneracy: there are still bands separated in energy by $\approx \hbar\omega$ in the energy spectrum as a function of l . These bands (shell structure) give, as in the $g = 0$ case, rise to the steplike structure of $\mu(N)$. For comparison, we have also in Fig. (3) plotted the non-interacting wave functions as dashed lines. As expected, we see that the effect of the interactions is to compress the quasiparticle states closer to the center of the trap where the Hartree field is large. The cloud of particles is compressed as will also be seen from the density distributions plotted in Sec. (VI). We can qualitatively understand the slight increase in energy with increasing l as seen from the solid lines in Fig. (2) (a). The low angular momentum functions have a larger amplitude in the center of the trap and are thus more affected by the Hartree field than the high l states.

Contrary to the $\mu = 8\hbar\omega$ case, we see from the solid lines in Fig. (2) (b), that when $\mu = 13\hbar\omega$ the approximate independence of the quasiparticle energies on l no longer holds. The Hartree field is now so strong that it has washed out the shell structure of the spectrum and it is qualitatively different from the $g = 0$ case. The energies now increase significantly with increasing l . This explains the fact from Fig. (1) (a), that for $\mu \sim 13$ and $g' = 2$ the steplike features have disappeared.

V. THE ENERGY AND THE HEAT CAPACITY

For a gas of particles in a constant confining potential, the most useful definition of the heat capacity is [12] is $C_N \equiv \frac{1}{2N} \partial E / \partial T|_N$ with $E(T, N)$ given by Eq. (6). As pointed out by Schneider and Wallis [8], the shell structure of the harmonic trap spectrum has a drastic consequence for the low temperature ($k_B T \ll \hbar\omega$) heat capacity; the gaps in the energy spectrum for $g = 0$ mean that the heat capacity is exponentially suppressed for low temperatures. In the non-interacting case the total energy for particles in both hyperfine states is given by

$$E(T) = 2 \sum_{\nu} E_{\nu} D_{\nu} f(E_{\nu}). \quad (9)$$

When the number of particles is such that a finite number of energy levels up to and including the level E_{ν_F} are completely filled for $T = 0$ (i.e. $N = 1, 4, 10, 20, \dots$ for $\nu_F = 0, 1, 2, 3, \dots$), the low temperature chemical potential for a constant number of particles is given by

$$\mu(T) = E_{\nu_F} + \frac{\hbar\omega}{2} - \frac{1}{2} \ln(\kappa_{\nu_F}) k_B T \quad (10)$$

with $\kappa_{\nu_F} = D_{\nu_F+1}/D_{\nu_F} > 1$. The low temperature heat capacity is then easily found to be

$$\frac{C_N(T)}{2Nk_B} = [(\nu_F + 5/2)D_{\nu_F+1} \frac{1}{\sqrt{\kappa_{\nu_F}}} - (\nu_F + 3/2)D_{\nu_F} \sqrt{\kappa_{\nu_F}}] \frac{(\hbar\omega)^2 e^{-\beta\hbar\omega/2}}{2N(k_B T)^2} \quad (11)$$

where $\beta = 1/k_B T$. This is, as one would expect, suppressed by a factor $\exp(-\beta\hbar\omega/2)$ as compared to the usual low temperature Thomas-Fermi result:

$$\frac{C_N(T)}{2Nk_B} = \frac{\pi^2 k_B T}{\hbar\omega(6N)^{1/3}}. \quad (12)$$

It is interesting to examine how the interactions change this result. In Fig. (4) we have plotted the energy per particle $E'/2N$ of the interacting gas as a function of temperature $T' \equiv T/\hbar\omega$, where $E' \equiv E/\hbar\omega$ and the energy is given by Eq. (6). We have used the parameters $g' = 0.4$, $N = 5456$ (a) and $g' = 0.4$, $N = 43680$ (b). For comparison we have also plotted the $g = 0$ results as dashed lines in Fig. (4) (c)-(d). As can be seen the interactions for both set of parameters have lowered the total energy of the gas considerably. This is as expected as we from Fig. (1) see, that the chemical potential in both cases is significantly lower than the $g = 0$ result. Fig. (5) depicts the corresponding heat capacity as a function of the temperature for $N = 5456$ (a) and $N = 43680$ (b) (solid lines). The dashed lines are the $g = 0$ results and the dash-dotted line is the Thomas-Fermi result for $g' = 0$ as given by Eq. (12). For $N = 5456$ (Fig. (5) (a)) we see, that the heat capacity for the interacting system is still exponentially suppressed for $k_B T \ll \hbar\omega$. For very low T the heat capacity is practically zero as for the $g = 0$ case and the interactions have not changed the qualitative behaviour of the heat capacity. This is a direct result of the fact that the interactions have not changed the shell structure of the energy spectrum. This can be seen from Fig. (1) (b)) where the step like features of $\mu(N)$ are still prevailing for $g' = 0.4$ and $N = 5456$.

The break-down of this effect is shown in Fig. (5) (b). We see that for $N = 43680$ the interactions have now increased heat capacity substantially over the non-interacting result for low temperatures. It has the same order of magnitude as the Thomas-Fermi prediction and it is qualitatively different from the non-interacting case. This is due to the fact that for this set of parameters the interactions have washed out the shell structure in the energy spectrum (the l -degeneracy) as can be seen from Fig. (1), where the steplike features are smoothed out for $N = 43680$ and $g' = 0.4$. There are no gaps of $\hbar\omega$ in the spectrum and hence no exponential damping factor in the heat capacity.

It should be noted that for very low temperatures the possibility of a transition to a superfluid state arises [4]. From the well known result of weak coupling superconductors, we expect that this transition will give rise to a kink in the $E(T)$ curve as the energy per particle is lowered as compared to the normal state [13]. From this kink, we obtain a discontinuity in $C_N(T)$ at the transition temperature T_c . We will not in this paper consider this effect as we are concentrating on the normal state behaviour. Work is under progress to examine for which temperatures and densities this transition takes place and how it can be determined experimentally.

We conclude, that the interactions in general lower the total energy as one would expect. The effect of the interaction on the heat capacity depends on the strength of the interactions and on the number of particles in the system. When few particles are in the system or when the interaction is so weak that the shell structure of the energy spectrum is intact, the heat capacity is still exponentially suppressed for low temperatures. The heat capacity can be suppressed although the total energy of the system is significantly lower than for the non-interacting case. This is, of course, a consequence of the fact that the lowering of the quasiparticle energies and the washing out of the shell structure happen at different set of parameters g and N as explained in Sec. III-IV. Once the interactions are strong enough to wash out the shell structure around the chemical potential, the behaviour of the heat capacity changes qualitatively. It is no longer suppressed and has the same order of magnitude as the Thomas-Fermi prediction. The transition between those two limiting behaviours is smooth as a function of N or g .

VI. DENSITY DISTRIBUTIONS

In this section we will present results for the density and momentum distributions. In an isotropic trap, these distributions will be spherically symmetric when the gas is in the ground state. The density distribution $\rho(r)$ is calculated from $\rho(r) = -U(r)/g$ with $U(r)$ given by Eq. (5). In Fig. (6), $\rho(r/l)$ is displayed for $N = 120, 165$ and $g' = 2$. For comparison we have also plotted the distributions for $g' = 0$. The dashed curves are the Thomas-Fermi results obtained from the solution of Eq. (7)-(8) with a given N . The temperature is taken to be zero. As can be seen, $\rho(r/l)$ is substantially changed due to the interactions. The cloud of particles is compressed as compared to the non-interacting result due to the attractive forces. As a high density of particles increases the critical temperature for a BCS-type transition, this effect favours the formation of the superfluid state [4]. Furthermore, we observe a central

minimum for $N = 120$ and a central peak for $N = 165$ for both $g' = 2$ and $g' = 0$ as compared to the Thomas-Fermi predictions. For the $g' = 0$, this is because $N = 165$ corresponds to a filled shell with $\nu_F = 8$, $N = 120$ corresponds to a filled shell with $\nu_F = 7$ and the fact that shells with $\nu = \text{odd}$ do not contribute to $\rho(0)$ as they have odd angular momentum [8]. We see that the interacting system exhibit the same qualitative dependence of $\rho(0)$ for this set of parameters, even though the actual densities are substantially different from their $g' = 0$ counterparts. This is due to the fact, that for this set of parameters, the shell structure of the quasiparticle spectrum is still intact although the actual energies and wave functions are changed substantially. This can be seen from Fig. (1) (a) where the step like features still prevail for this set of parameters. Thus, even for $g' = 2$, $N = 165$ still corresponds a highest shell of even angular momentum states totally filled whereas $N = 120$ corresponds a filled highest shell of odd angular momentum states. For a larger number of particles, where the shell structure of the quasiparticle spectrum has been washed out, it turns out that this behaviour of $\rho(0)$ has disappeared as expected. Also, a non-vanishing temperature will tend to wash out the predicted dip/top behaviour of the density as the transition from occupied to unoccupied shells as a function of energy becomes less abrupt.

The momentum distribution of the particles is not completely straightforward to measure. A simple free expansion experiment where one switches off the trap potential non-adiabatically does not strictly measure this distribution. The reason is, that the gas does not expand freely; collisions between particles in different hyperfine states will alter the momentum distribution. One would need a time-dependent formalism [14] in order to treat such an expansion rigorously. However, we will here assume that the momentum distribution in the trapped state gives a good indication of the distribution measured in such a free expansion experiment. The spherically symmetric momentum distribution $\langle c_k^\dagger c_k \rangle$, where c_k^\dagger creates a particle in a plane wave state $\exp(ikz)$ along an arbitrary z -direction, is calculated from

$$\langle c_k^\dagger c_k \rangle = \sum_{\nu l} |\langle k | u_{l0}^\nu \rangle|^2 f(E_l^\nu). \quad (13)$$

Here we have utilized the fact, that a plane wave along the z -direction only contains $m = 0$ spherical harmonics. Using the well known expansion of a plane wave $\exp(ikz)$ in spherical harmonics [15] we obtain

$$\begin{aligned} \langle k | u_{l0}^\nu \rangle &= \int d^3r e^{-ikz} u_{l0}^\nu(\mathbf{r}) \\ &= (-i)^l \sqrt{(2l+1)4\pi} \left(\frac{\pi}{2k}\right)^{1/2} \int_0^\infty J_{l+1/2}(kr) u_l^\nu(r) \sqrt{r} dr \end{aligned} \quad (14)$$

where $J_{l+1/2}(x)$ is the ordinary Bessel function. In Fig. (7), we have plotted the momentum distribution for $N = 43680$ and $g' = 0.4$. The momentum is measured in units of l^{-1} . The dashed curve is the non-interacting result. For this high number of particles, the shell structure of the quasiparticle spectrum is washed out and the distributions are, apart from a small shell around the edge of the cloud, almost identical to the Thomas-Fermi prediction (not plotted). We see that the interactions have spread out the distribution considerably as compared to the non-interacting case. As the Hartree field lowers the quasiparticle energies more levels become occupied in the center of the trap. The higher momentum states thus become populated leading to a spreading out of the momentum distribution as compared to the $g' = 0$ case.

We conclude that the interactions in general alter both the momentum distribution and the density distribution substantially. The density distribution is compressed and the momentum distribution spread out as compared to the non-interacting results. Furthermore, the central minima and maxima of $\rho(r)$ as a function of N can still be observed, when the interactions have not yet washed out the shell structure of the quasiparticle spectrum.

VII. CONCLUSION

In this paper we have considered a trapped spin-polarized gas of interacting fermions. We find that the interactions have two distinct effects on the quasiparticle spectrum. It lowers the quasiparticle energies and thus the total energy of the gas. Also, above a certain number of particles in the trap, it washes out the shell like structure of the spectrum associated with a harmonic trap. These two effects are independent, in the sense that the energy of the gas can be lowered considerably as compared to the non-interacting case, but the shell structure of the spectrum is left relatively intact. One can still, therefore, observe effects such as step like features in the chemical potential, exponential damping of the low temperature heat capacity and maxima and minima in $\rho(0)$ associated with a non-interacting gas. Whether these effects will be observable depend on whether the condition $k_B T \ll \hbar\omega$ is experimentally feasible. The interactions are also found to compress the atom cloud and spread out the momentum distribution considerably. This effect should be readily observable; it is important to include in any realistic calculation of the properties of spin-polarized ${}^6\text{Li}$ in a trap.

VIII. ACKNOWLEDGMENTS

This work was supported by the Engineering and Physical Sciences Research Council. We should also like to acknowledge valuable discussions with R. Dum.

- [1] M. H. Anderson, J. R. Ensher, M. R. Matthews, C. E. Wieman, and E. A. Cornell, *Science* **269**, 198 (1995)
- [2] C. C. Bradley, C. A. Sackett, J. J. Tollet, and R. G. Hulet, *Phys. Rev. Lett.* **75**, 1687 (1995); C. C. Bradley, C. A. Sackett, and R. G. Hulet, *Phys. Rev. Lett.* **78**, 985 (1997)
- [3] K. B. Davis, M. O. Mewes, M. R. Andrews, N. J. van Druten, D. S. Durfee, D. M. Kurn, and W. Ketterle, *Phys. Rev. Lett.* **75**, 3969 (1995)
- [4] H. T. C. Stoof, M. Houbiers, C. A. Sackett, and R. G. Hulet, *Phys. Rev. Lett.* **76**, 10 (1996)
- [5] E. R. I. Abraham, W. I. McAlexander, J. M. Gerton, R. G. Hulet, R. Côté, and A. Dalgarno, *Phys. Rev. A* **55**, R3299 (1997)
- [6] M. Houbiers, R. Ferwerda, H. T. C. Stoof, W. I. McAlexander, C. A. Sackett, and R. G. Hulet, *Phys. Rev. A* **56**, 4864 (1997)
- [7] D. A. Butts and D. S. Rokhsar, *Phys. Rev. A* **55**, 4346 (1997)
- [8] J. Schneider and H. Wallis, *Phys. Rev. A* **57**, 1253 (1998)
- [9] H. T. C. Stoof, *Phys. Rev. A* **49**, 3824 (1994)
- [10] D. S. Jin, M. R. Matthews, J. R. Ensher, C. E. Wieman, and E. A. Cornell, *Phys. Rev. Lett.* **78**, 764 (1997)
- [11] M. O. Mewes, M. R. Andrews, N. J. van Druten, D. M. Kurn, D. S. Durfee, C. G. Townsend, and W. Ketterle, *Phys. Rev. Lett.* **77**, 988 (1996)
- [12] J. R. Ensher, D. S. Jin, M. R. Matthews, C. E. Wieman, and E. A. Cornell, *Phys. Rev. Lett.* **77**, 4984 (1997)
- [13] M. Tinkham, *Introduction to Superconductivity* (McGraw-Hill, New York, 1975)
- [14] M. Holland and J. Cooper, *Phys. Rev. A* **53**, R1954 (1996)
- [15] See, for instance, L. I. Schiff, *Quantum Mechanics* (McGraw-Hill, New York, 1968)

Figure Captions

Fig. 1: $\mu(N_\sigma)$ in units of $\hbar\omega$ for $g' = 1, g' = 2$ (a) and $g' = 0.2, g' = 0.4$ (b). The dashed lines are the Thomas-Fermi approximation.

Fig. 2: The quasiparticle spectrum in units of $\hbar\omega$ for $g' = 2, \mu/\hbar\omega = 8$ (a) and $g' = 2, \mu/\hbar\omega = 13$ (b).

Fig. 3: The radial quasiparticle wave functions for $\nu = 8, l = 0$ (a) and $\nu = 8, l = 8$ (b) as a function of r/l . The solid lines are for $g' = 2$ and the dashed lines are for $g' = 0$. The Hartree field in units of $\hbar\omega$ is plotted in (c).

Fig. 4: The energy in units of $\hbar\omega$ for $g' = 0.4$ (solid lines) and $N = 5456$ (a) and $N = 43680$ (b). The dashed lines in are for the non-interacting case for $N = 5456$ (c) and $N = 43680$ (d).

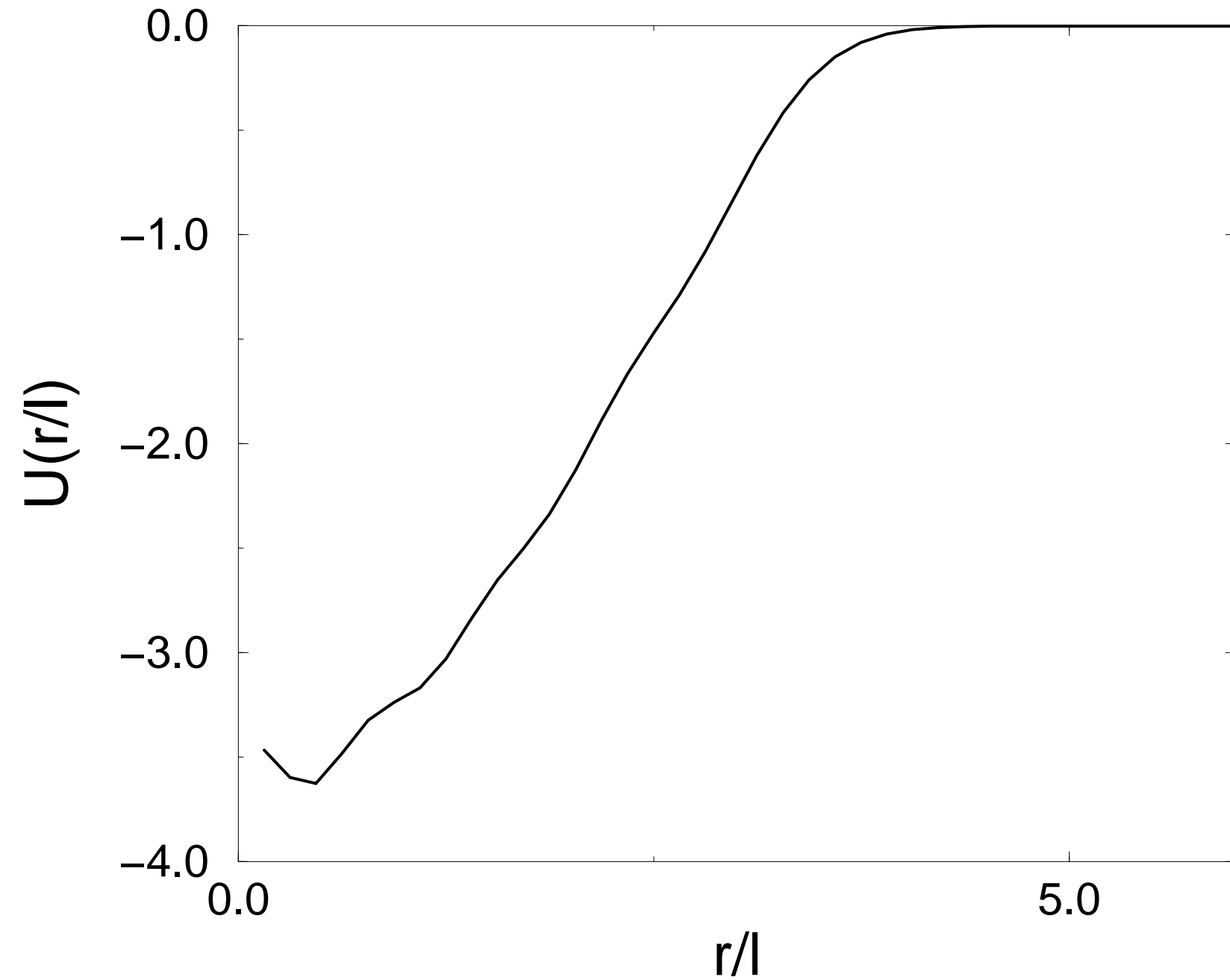
Fig. 5: The heat capacity in units of k_B for $g' = 0.4$ and $N = 5456$ (a) and $N = 43680$ (b).

Fig. 6: The density distribution $\rho(r/l)$ for $N = 120, 165, g' = 0, 2$ (solid lines). The dashed lines are the Thomas-Fermi results.

Fig. 7: The momentum distribution $\langle c_k^\dagger c_k \rangle$ for $N = 43680, g' = 0.4$ (solid) and $N = 43680, g' = 0.0$ (dashed)

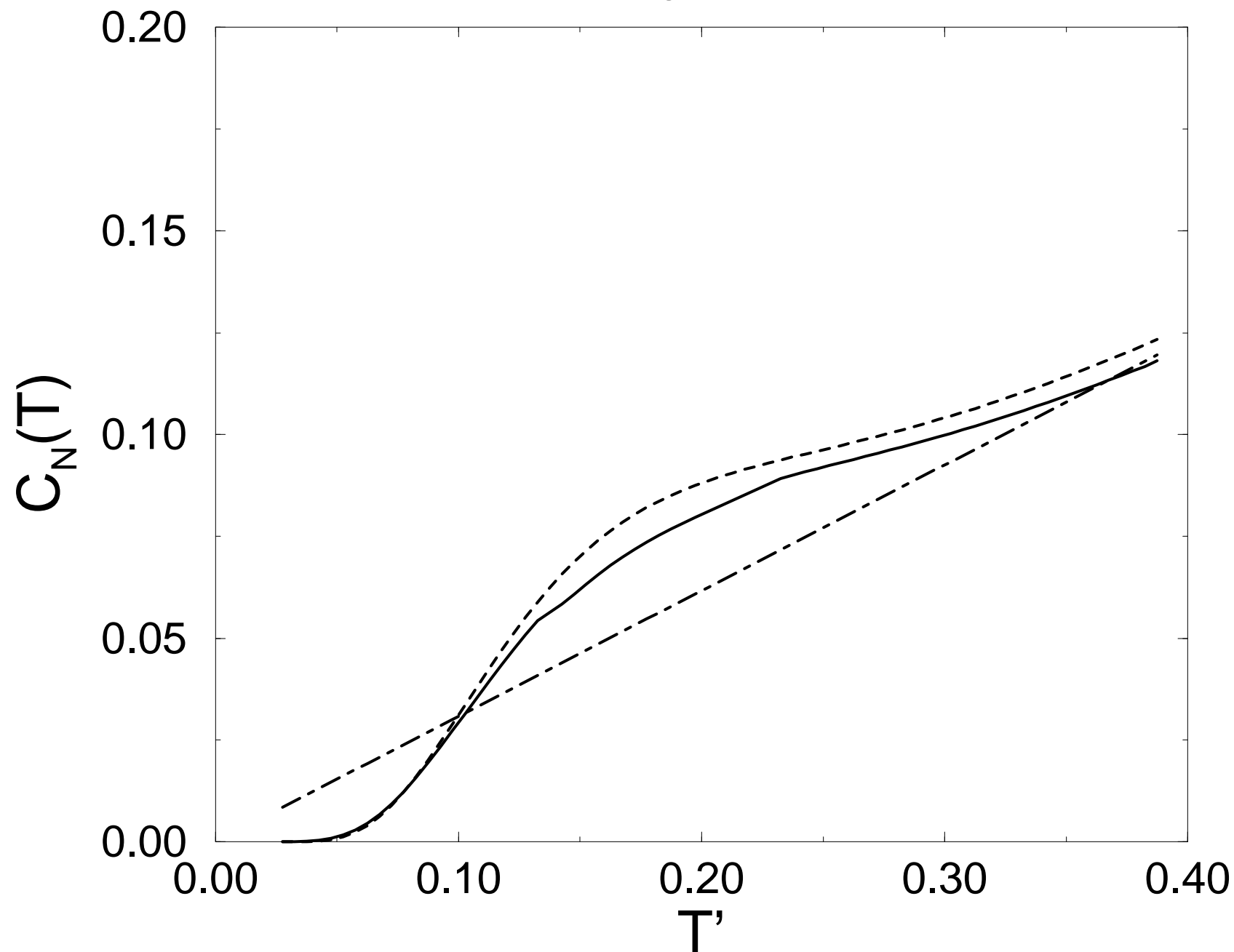
Bruun PRA

Fig.3 (c)



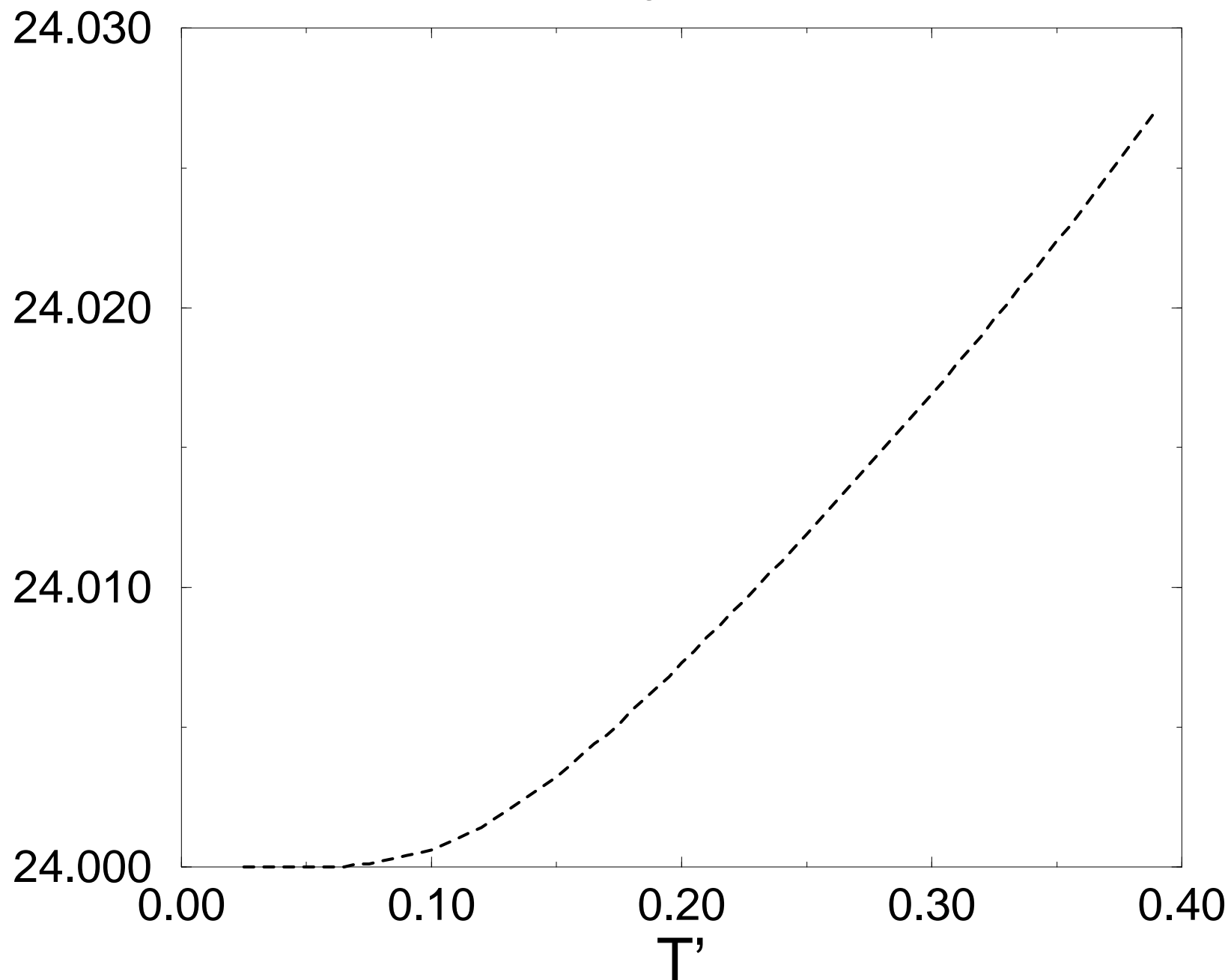
Bruun PRA

Fig.5 (a)



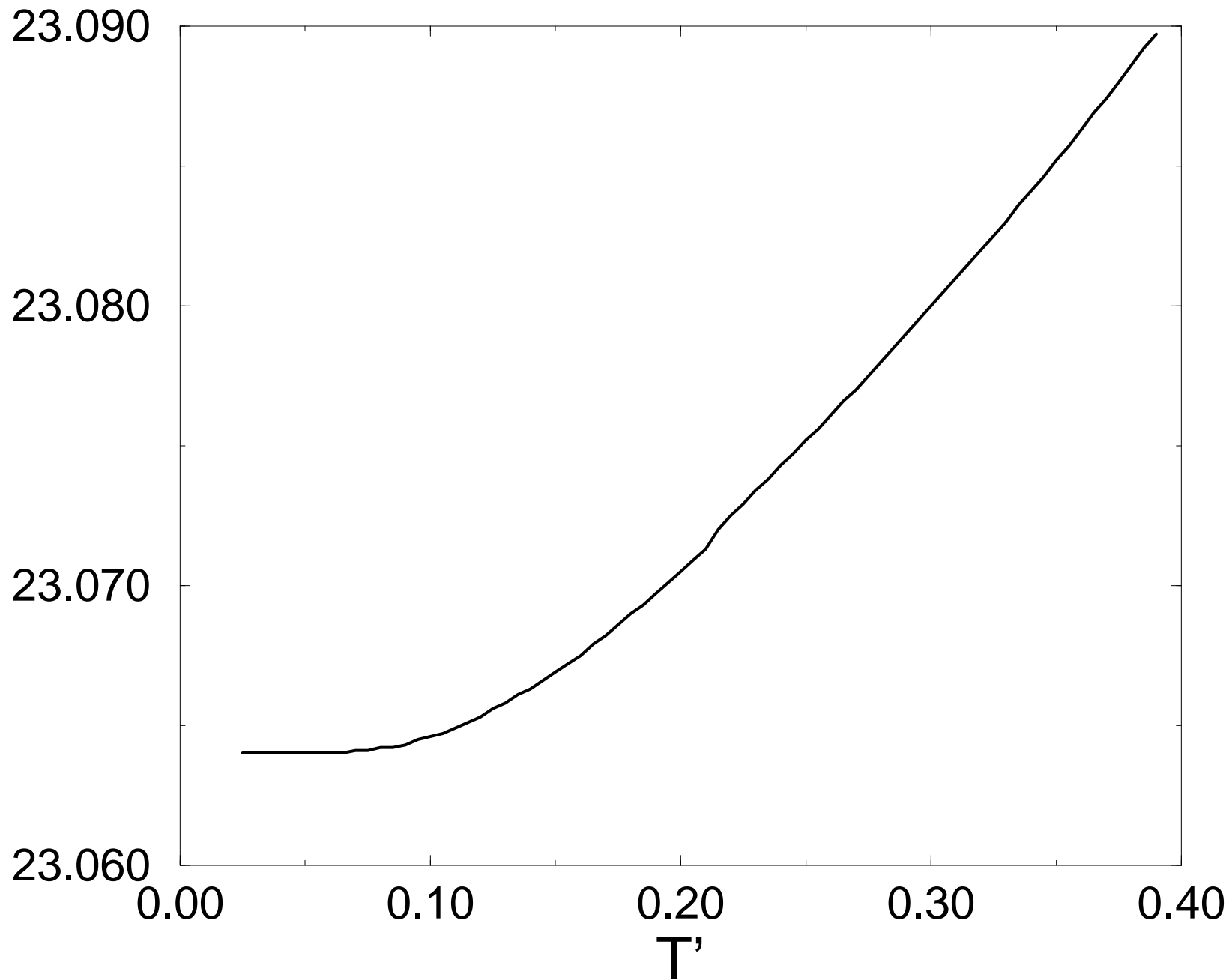
Bruun PRA

Fig.4 (c)



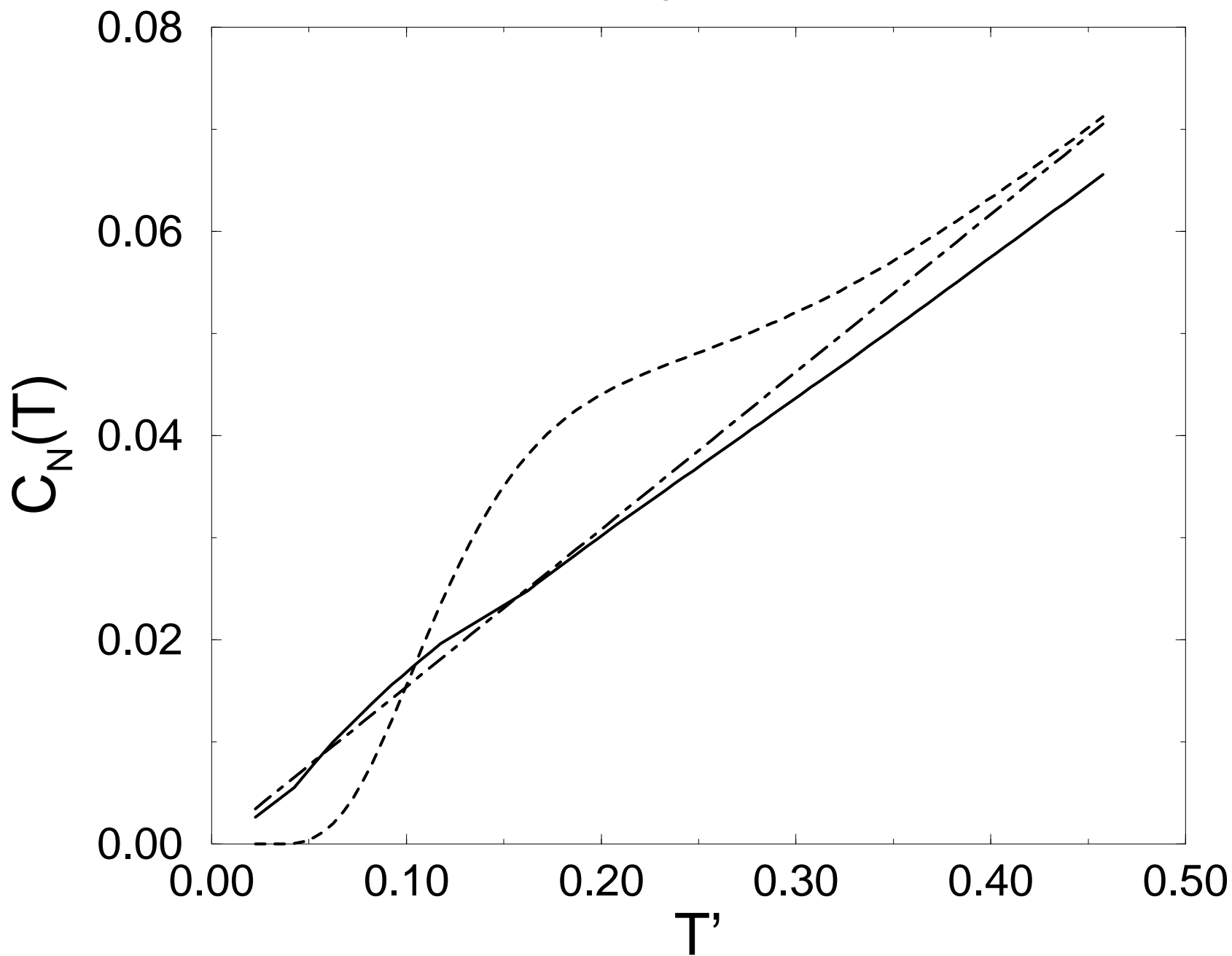
Bruun PRA

Fig.4 (a)



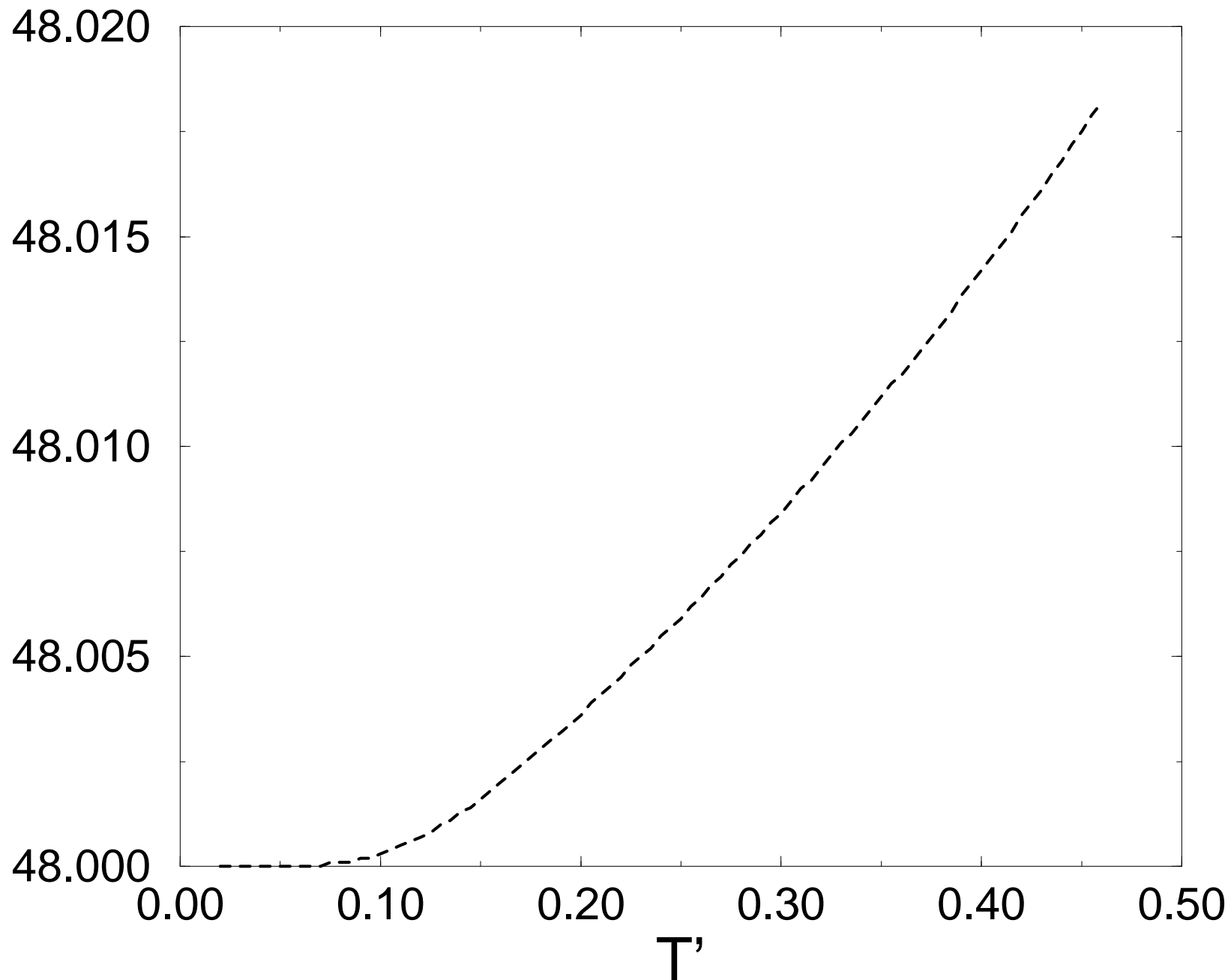
Bruun PRA

Fig.5 (b)



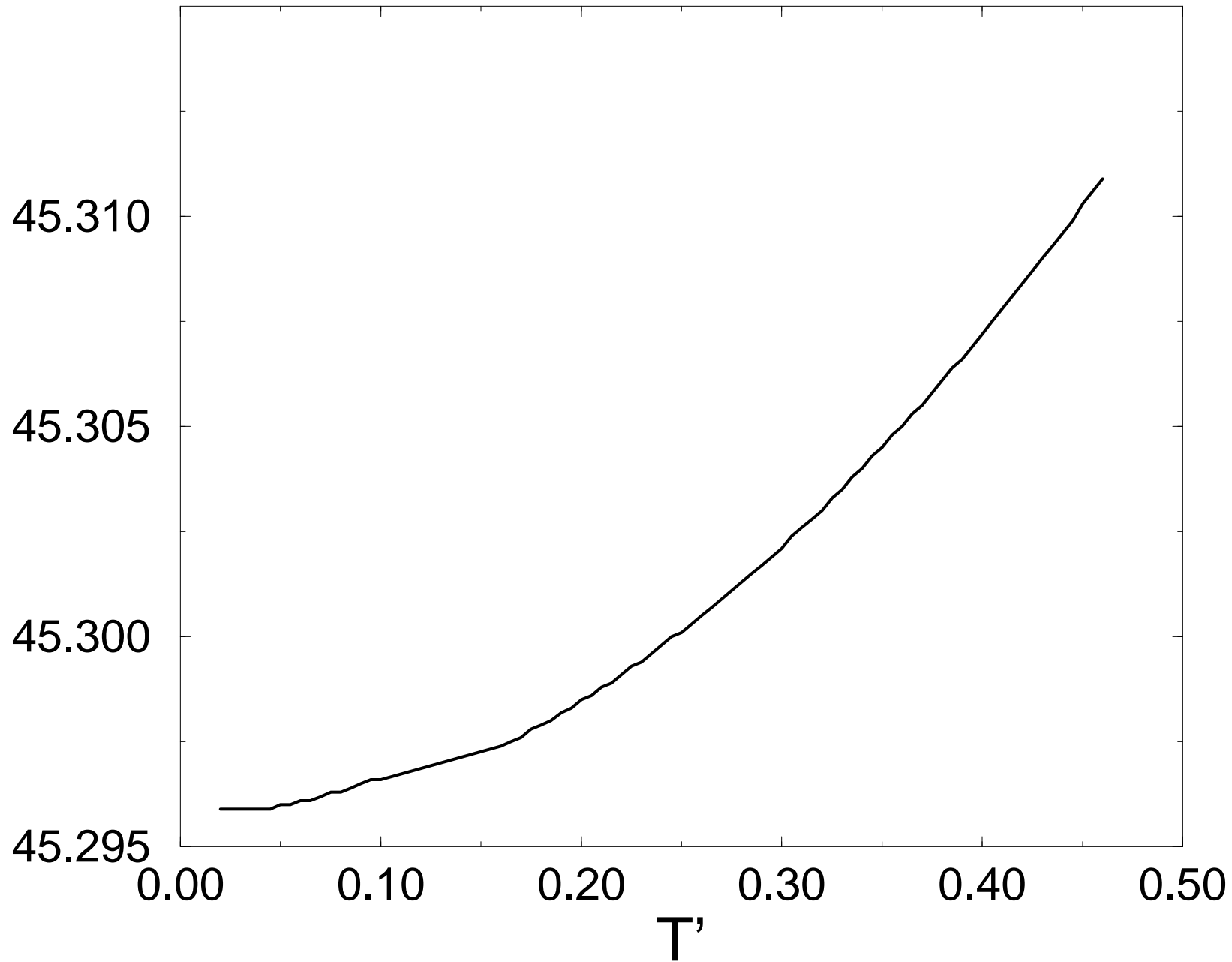
Bruun PRA

Fig.4 (d)



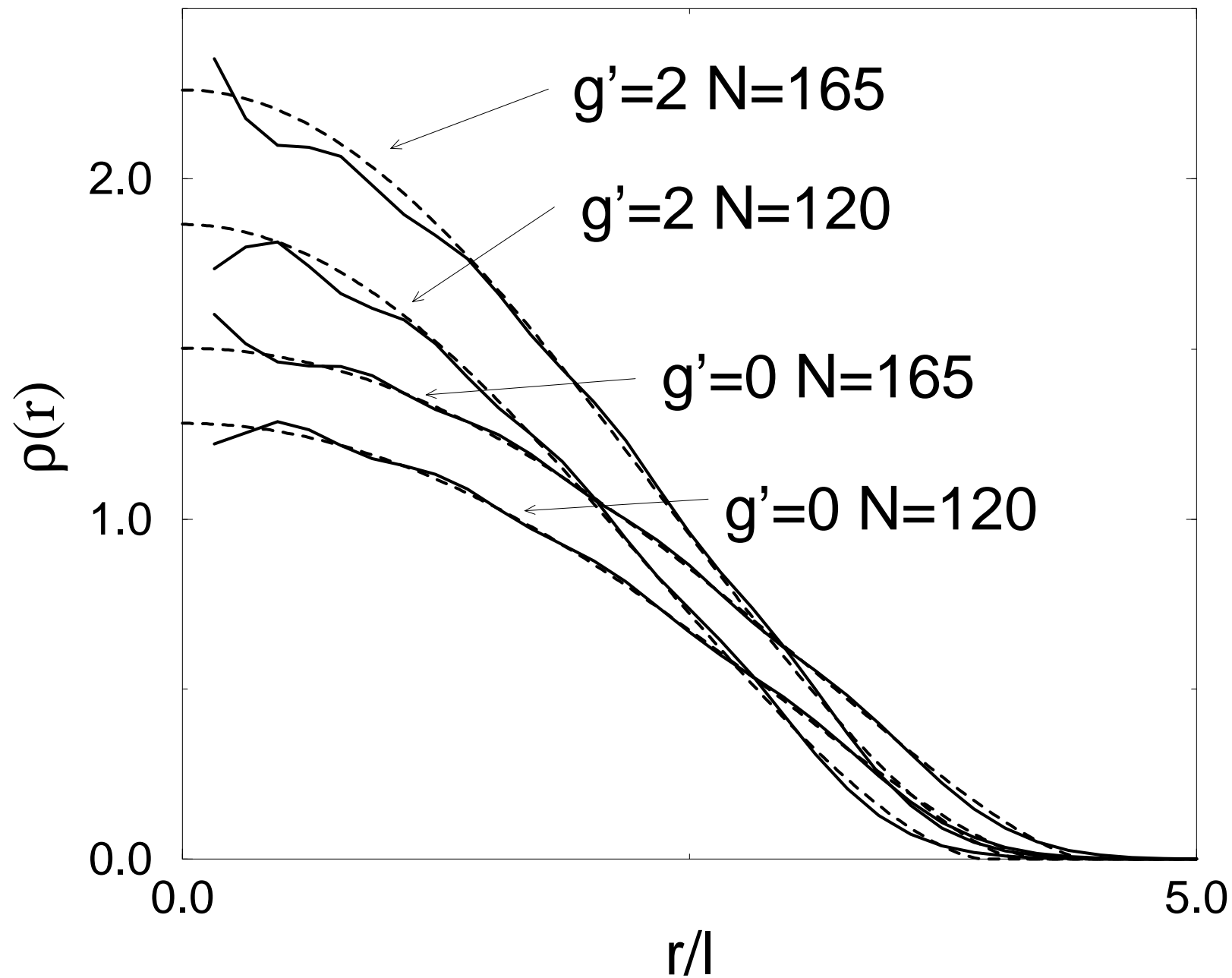
Bruun PRA

Fig.4 (b)



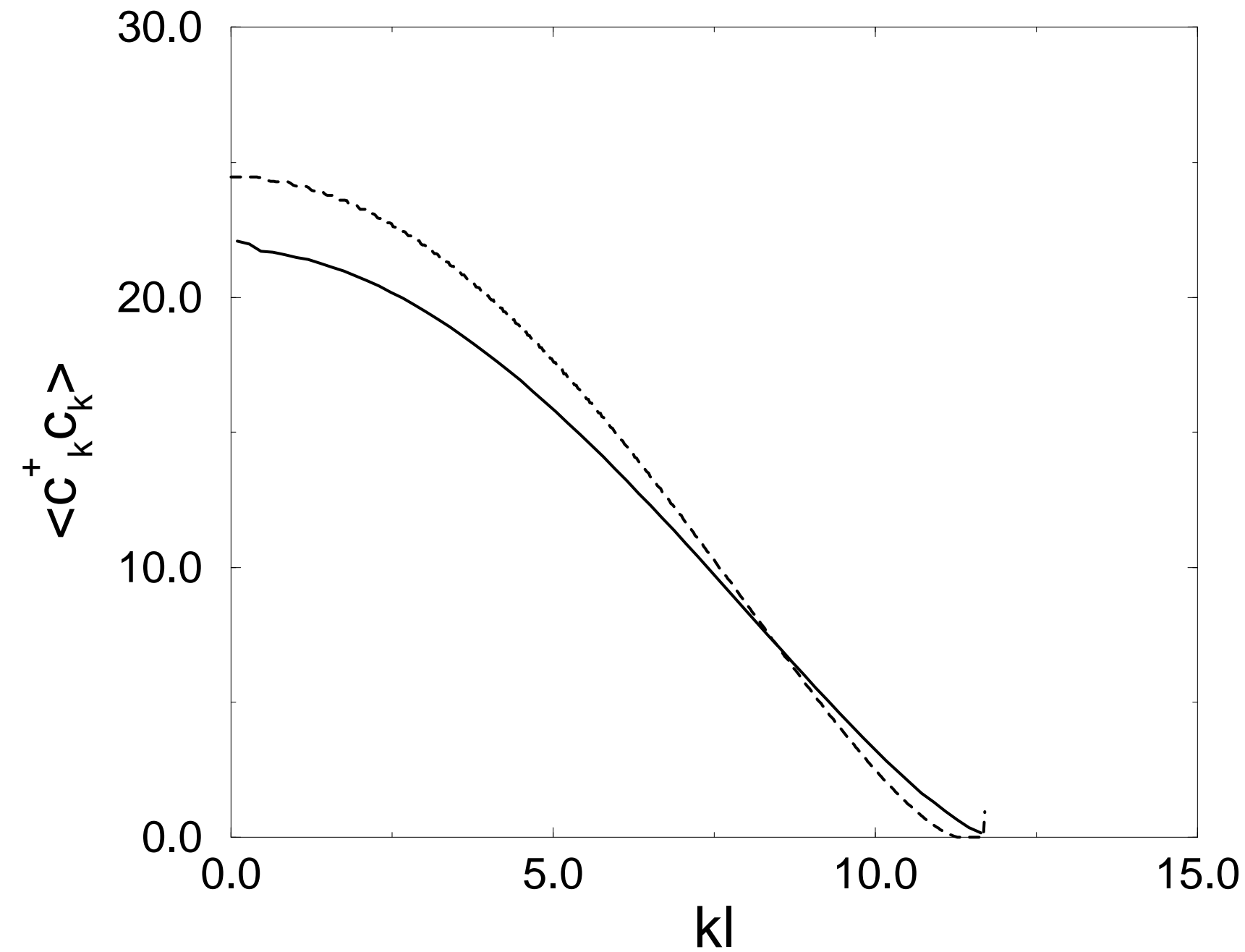
Bruun PRA

Fig. 6



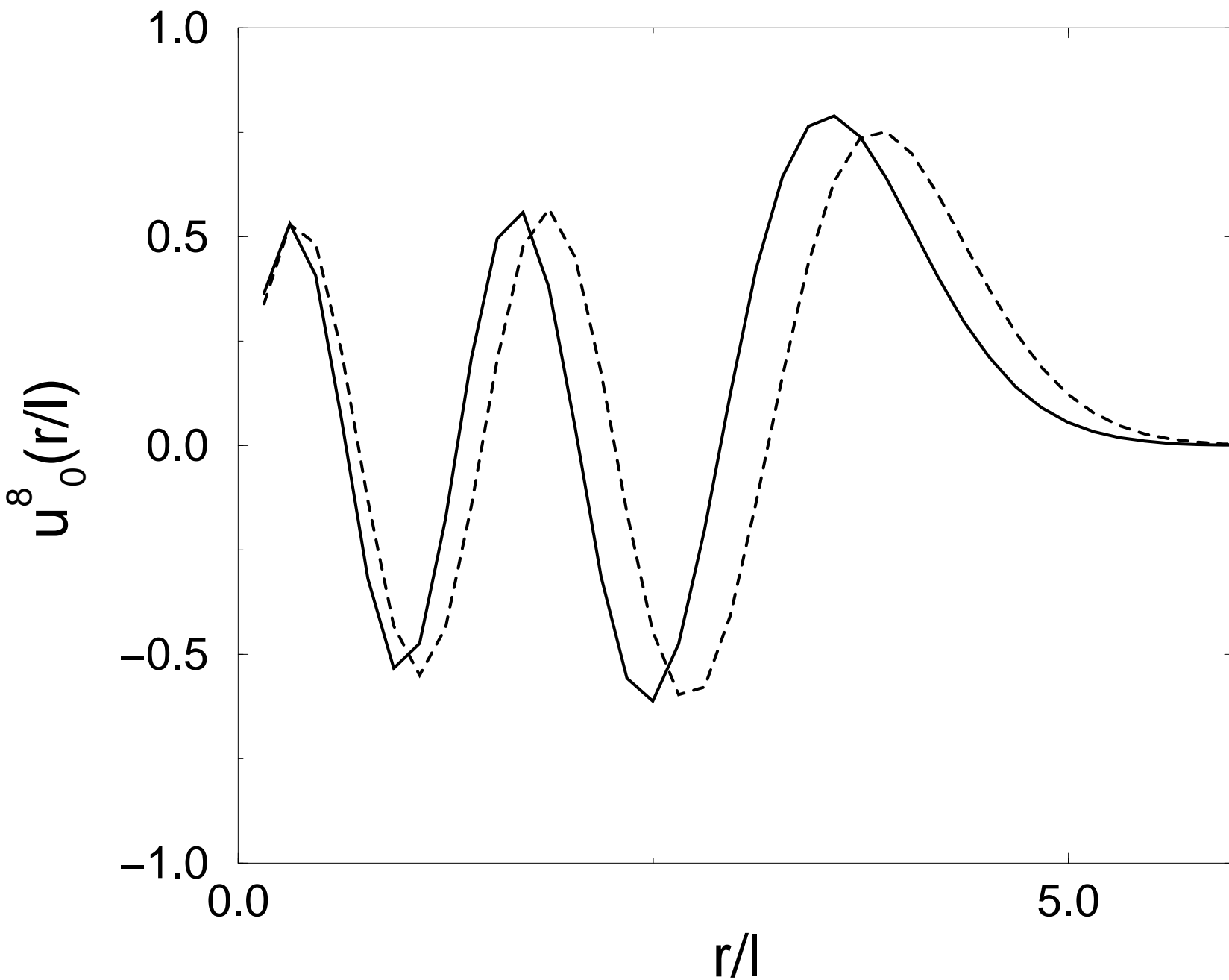
Bruun PRA

Fig. 7



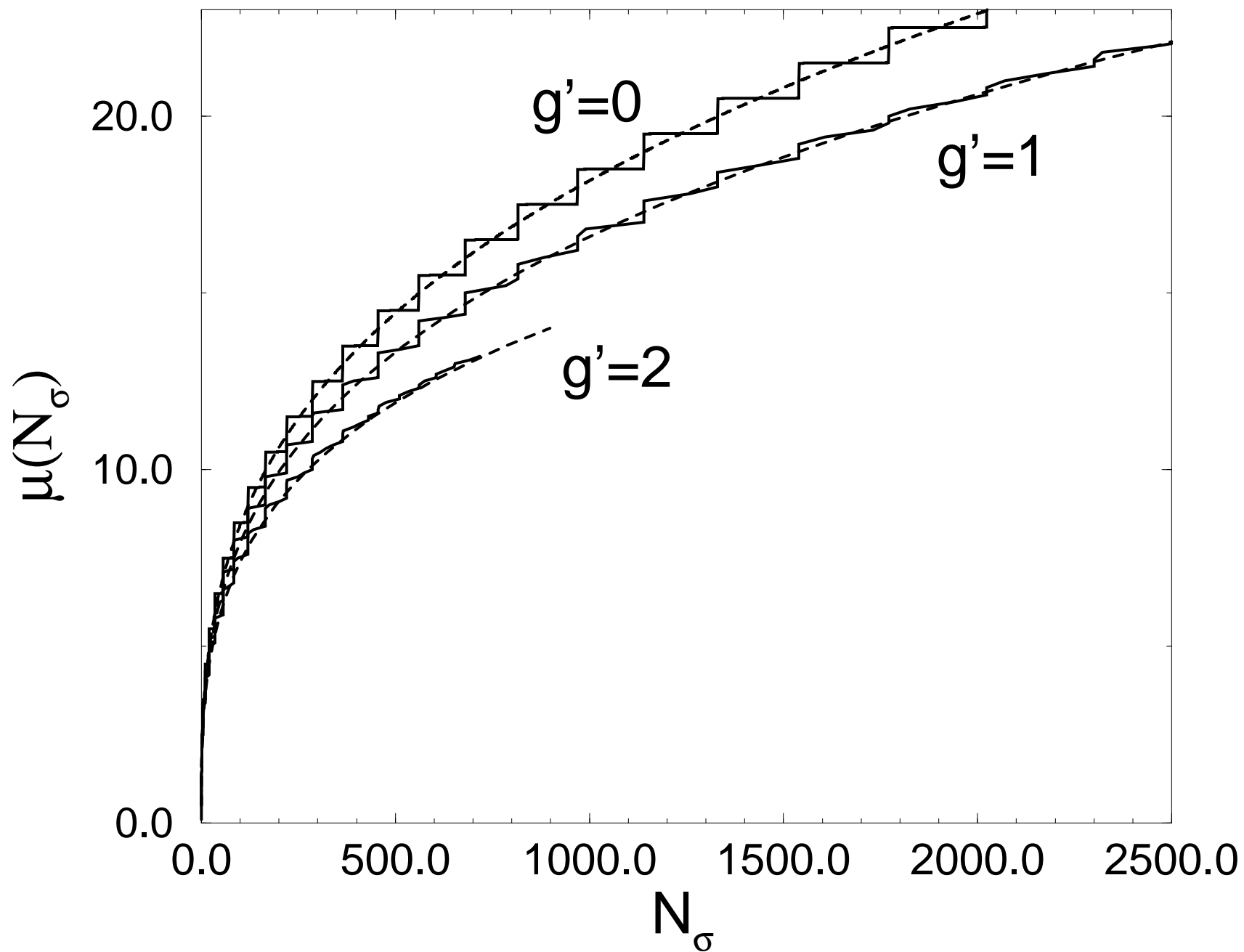
Bruun PRA

Fig.3 (a)



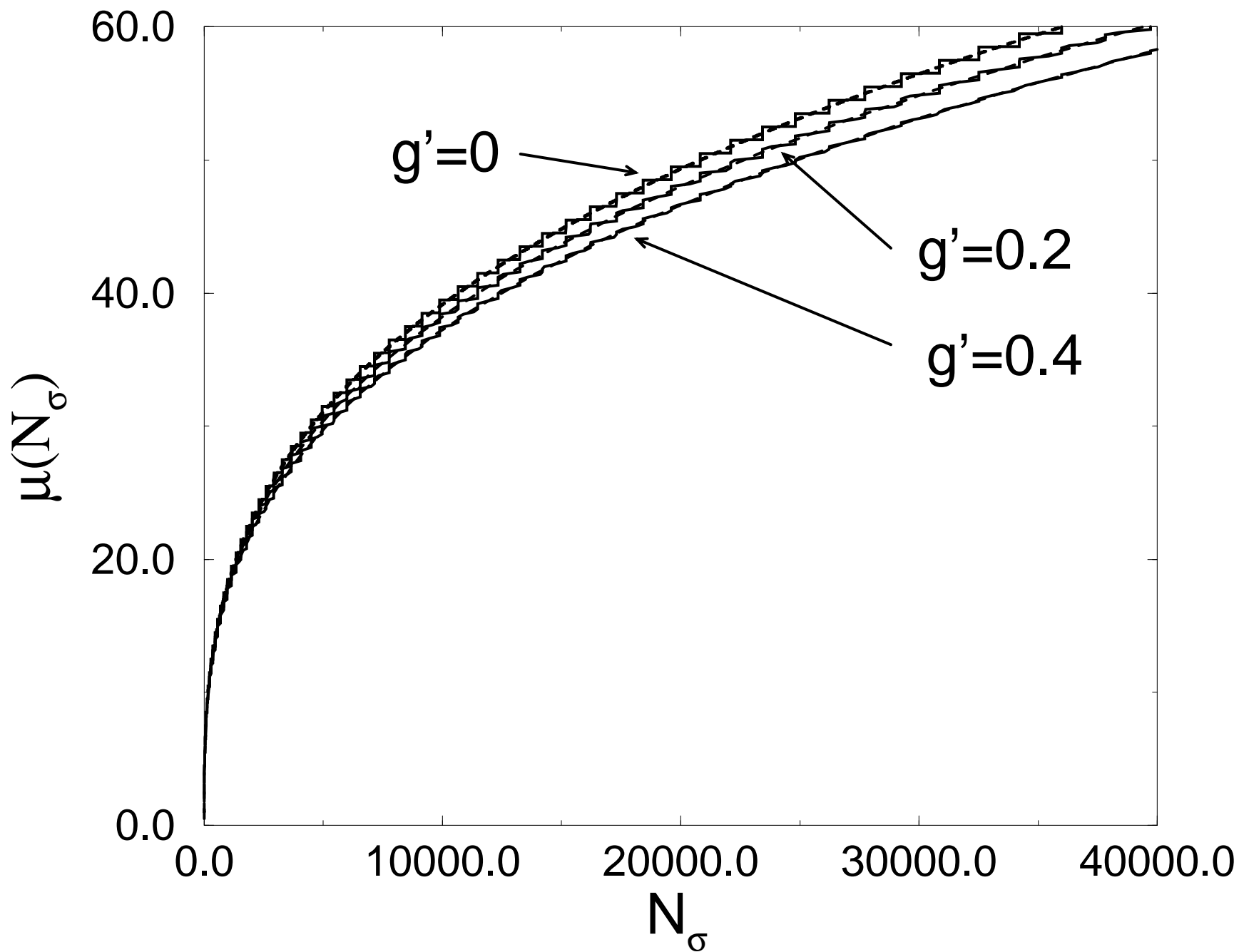
Bruun PRA

Fig.1 (a)



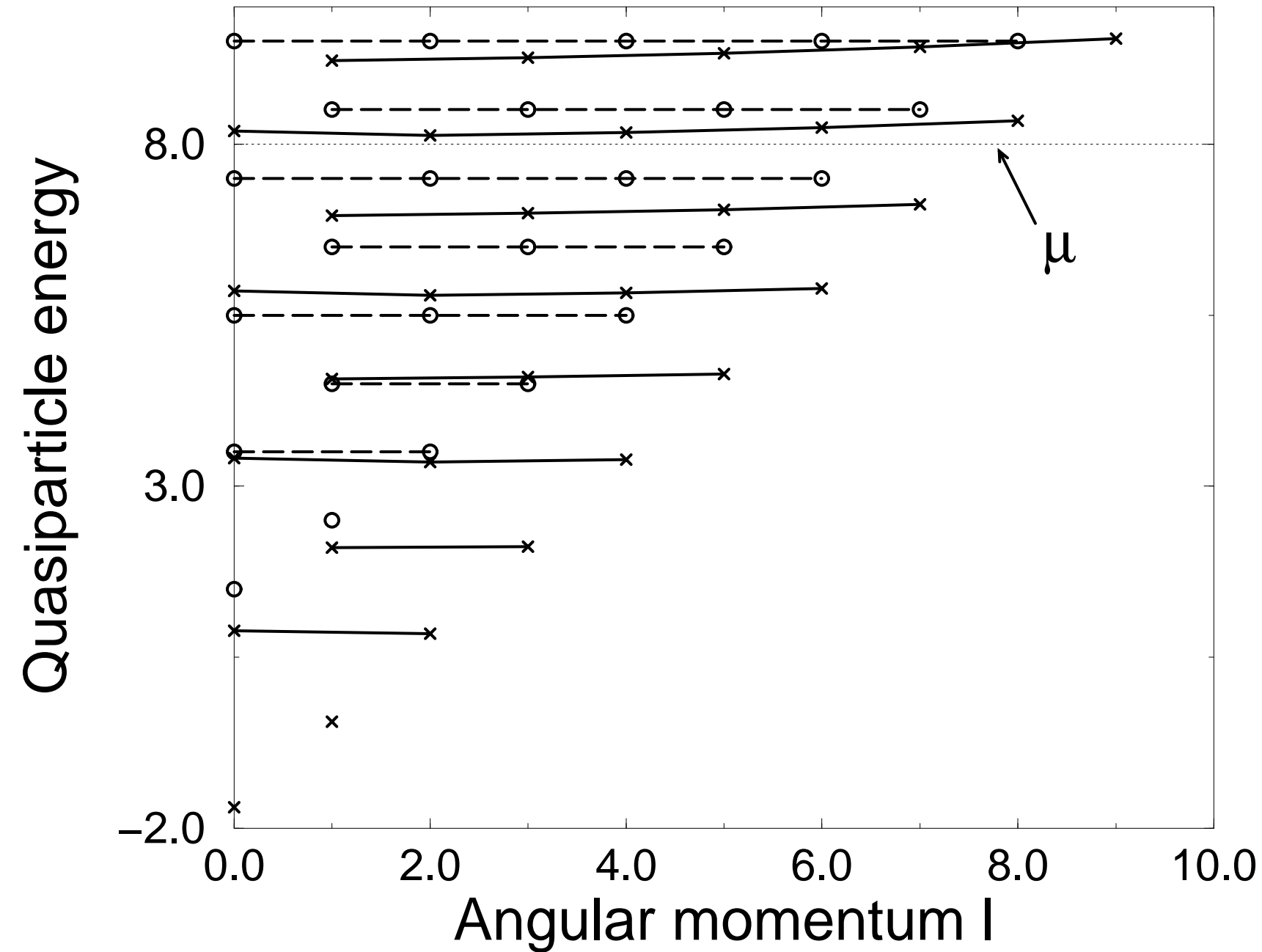
Bruun PRA

Fig.1 (b)



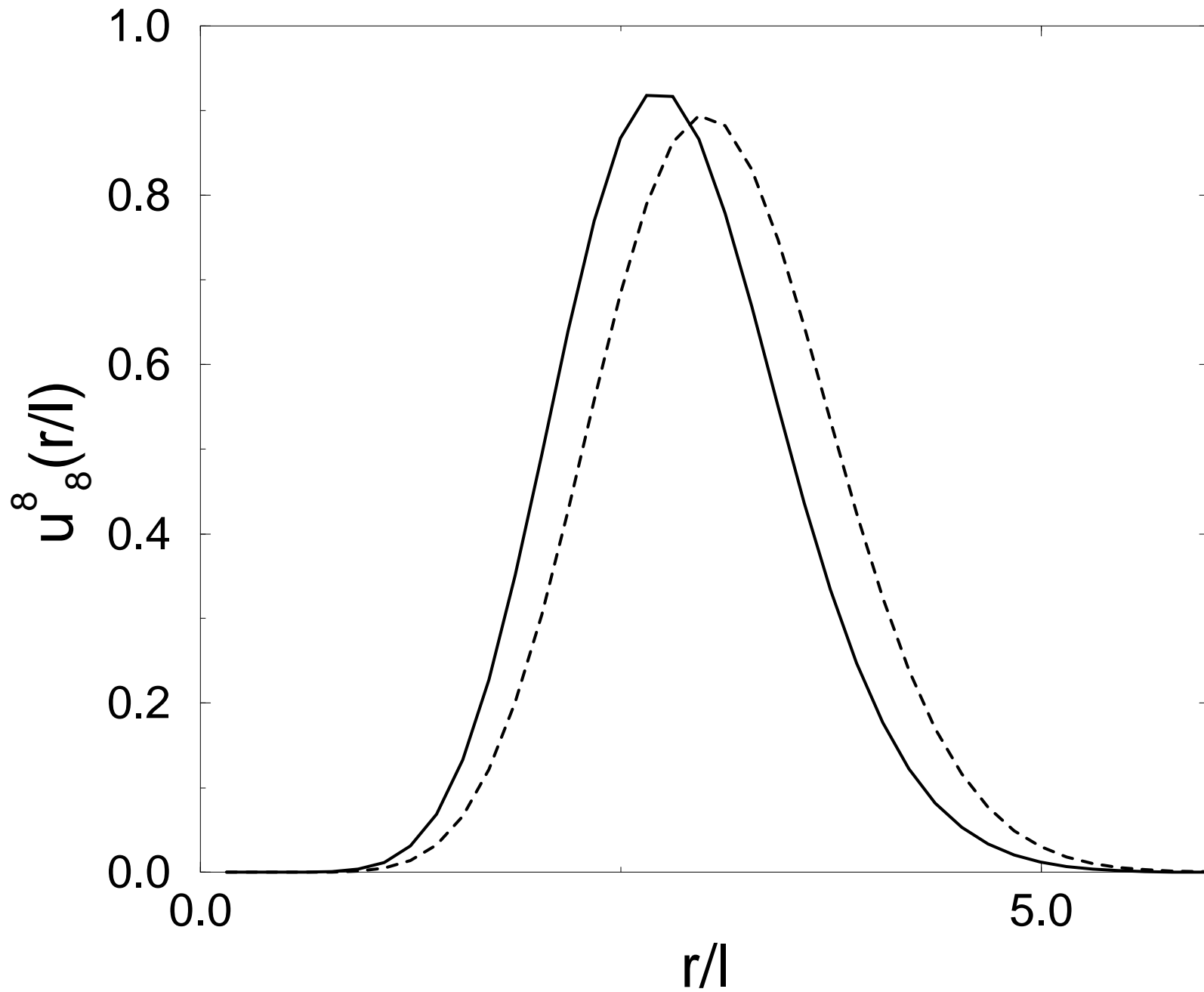
Bruun PRA

Fig.2 (a)



Bruun PRA

Fig.3 (b)



Bruun PRA

Fig.2 (b)

